REVIEWS

Journal of Semiconductors
(2019) 40, 111602
doi: 10.1088/1674-4926/40/11/111602

Recent advances in flexible photodetectors based on 1D nanostructures

Senpo Yip[1, 2], Lifan Shen[1, 3], and Johnny C Ho[1, 2, †]

[1]Department of Materials Science and Engineering, City University of Hong Kong, Hong Kong, China

[2]Shenzhen Research Institute, City University of Hong Kong, Shenzhen 518057, China

[3]College of Microelectronics and Key Laboratory of Optoelectronics Technology, Faculty of Information Technology, Beijing University of Technology, Beijing 100124, China

Abstract: Semiconductor nanowires have demonstrated excellent electronic and optoelectronic properties. When integrated into photodetectors, excellent device performance can be easily attained. Apart from the exceptional performance, these nanowires can also enable robust and mechanically flexible photodetectors for various advanced utilizations that the rigid counterparts cannot perform. These unique applications include personal healthcare, next-generation robotics and many others. In this review, we would first discuss the nanowire fabrication techniques as well as the assembly methods of constructing large-scale nanowire arrays. Then, the recent development of flexible photodetectors based on these different nanowire material systems is evaluated in detail. At the same time, we also introduce some recent advancement that allows individual photodetectors to integrate into a more complex system for advanced deployment. Finally, a short conclusion and outlook of challenges faced in the future of the community is presented.

Key words: nanowires; flexible; photodetectors

Citation: S P Yip, L F Shen, and J C Ho, Recent advances in flexible photodetectors based on 1D nanostructures[J]. *J. Semicond.*, 2019, 40(11), 111602. http://doi.org/10.1088/1674-4926/40/11/111602

1. Introduction

In the past few decades, the development of semiconductor devices has reshaped our lifestyle. One of the major advancements is the development of sensor that can response with the change of the environment. Among different types of sensors, photodetector is an optoelectronic device that transform light signal to electric signal. Upon the illumination of a light source, the electricity passes through the photodetector changes. Photodetector has found applications in different categories, from flame and smoke detection[1] to healthcare[2] and from military to wireless communication[3].

In general, photodetectors are built on rigid substrate like bulk silicon. The limitation of the rigid photodetector is that when undergo even a small deformation, the photodetector will crack and cannot function properly. Also, rigid sensor cannot be used on curved surface and hence restrict the usage in certain area like body temperature monitoring[4]. So, a photodetector that can be bent or twisted to a certain degree is necessary to be developed for some special applications.

A photodetector is typically constructed with a photosensing channel and two electrodes at the both ends of the channel. The sensing materials can be a bulk film or nanostructures like nanosheets, nanowires (NWs), nanotubes (NTs) or quantum dots (QDs). Among them, the 1D nanostructures like NWs and NTs exhibit some special properties like large surface-to-volume ratio that can enhance the photoresponse compare to their bulk counterparts. Also, due to the low dimensional feature, 1D nanostructure can withstand larger bending without cracking compares to their bulk counterparts. These features make the 1D nanostructure one of the ideal candidates to be integrated into flexible photodetector. In recent years, there are various attempts to develop NW-based flexible photodetector, from the material selection, fabrication and assembly techniques, to device fabrication and integrating them into a more complicated system for potential real-life application. In this review, the recent progress of NW fabrication and assembly techniques for flexible electronics are first reviewed. After that, some recent research progress is presented based on different material groups. Then the reports on integration of the flexible NW photodetector to more complicated system are introduced.

1.1. Types of photodetector

Before reviewing the recent progress, the background information would be first introduced. Firstly, some common types of photodetector are briefly introduced here. Photodetector can be classified as three groups based on their working principles. They are:

a) Photoconductor type: in which the excessive free charges is generated by absorption of photons. Those excessive charges increase the overall conductivity of the photodetector channel. Usually composed by a semiconductor channel as the sensing materials and two ohmic contacts as the source and drain for charges transfer.

b) Photovoltaic type: in which a built-in electric field is existed within the photodetector without illumination. This can be done by building a p–n junction within the sensing channel or a Schottky barrier junction between the contact and

Correspondence to: J C Ho, johnnyho@cityu.edu.hk
Received 21 JULY 2019.
©2019 Chinese Institute of Electronics

the semiconductor interface. Upon the illumination, the built-in electric field separates the photo-induced electron–hole pair and hence the generation of photocurrent.

c) Photogating type: in which an electric field is generated under the illumination. There are two types of mechanisms for the photogating effect generation. One is the photo-induced charges are trapped by the defects and the other is trapped by the surface absorbates. The trapped charges act as a local gate and modulate the current flow along the photodetector upon the illumination.

Different types of photodetectors have their individual advantage for applications. For example, photovoltaic type can be used to constructed self-powered photodetector which can reduce the total weight of the sensing unit as no external power source is needed[5]. One should also be reminded that here we just introduced those mechanism briefly and there are other photosensing mechanism[6–8]. Refs. [6–8] are referred if one want to have more information.

1.2. Figure of merits

Another important background information is the performance figure of merit for assessing the photodetector. With these figure-of-merits, the performance of different photodetector can be compared. There are several figure-of-merits that are frequently used for assessing photodetector and briefly introduced here.

Responsivity (R): Responsivity is a description of the efficiency of charge/voltage generation under illumination. It is the measured photocurrent or photovoltage divided by the power of the illumination source on the active area of the sensing material. It can be expressed as:

$$R = \frac{I \text{ or } V}{P}, \tag{1}$$

where I and V are photocurrent and photovoltage respectively, and P is the illumination source power.

External quantum efficiency (EQE): The EQE is the ratio of the total generated electron pairs which contribute the photocurrent and the total numbers of incident photons. The EQE can be expressed as:

$$\text{EQE} = \frac{I/e}{P/hv} = R\frac{hc}{e\lambda}, \tag{2}$$

where e is the elementary charge, h is Planck's constant, v is the frequency of incident light, c is the speed of incident light, and λ is the wavelength of incident light.

Response speed: Response speed is used to describe how fast a photodetector response upon the light illumination. It is usually described as two values: one is rise time and the other is the decay time. They are defined as the time used for the photocurrent to rise from 10% of the peak photocurrent to the 90% of the peak photocurrent for the rise time, and the time used for the photocurrent to drop from 90% of the peak photocurrent to the 10% of the peak photocurrent for the decay time.

Detectivity (D): Detectivity is used to describe the ability to detect signal from noise. It can be expressed as:

$$D = \frac{I}{p\sqrt{2qI_{\text{dark}}}}, \tag{3}$$

where q is the light intensity and I_{dark} is the dark current of the photodetector.

2. NW growth and assembly method for flexible electronics

2.1. Nanowire growth method

This part of the review will briefly introduce some NW fabrication techniques. Each technique has its own advantages and disadvantages. Basically, NW fabrication can be divided into two major categories, namely the "top–down" and the "bottom-up" approaches. The top–down approach means the NWs are fabricated from bulk materials and thin down the sizes and dimensionality. It is a simple and relatively straightforward method that involves material removal from a thin or thick film. Patterning is needed prior to the NW synthesis in order to define the NW position, shape and dimension. Material removal is performed by chemical etching or plasma etching. One example is metal-assisted chemical etching (MacEtch), which uses a patterned metal film as the catalyst to etch the substrate isotropically in order to create a high aspect-ratio structure[9, 10]. For instance, periodic high aspect-ratio GaAs NW arrays are produced by MacEtch by using n-type (100) GaAs substrates and Au catalyst films patterned with soft lithography[9]. The Si-doped (100) GaAs substrates are used as substrate, and potassium permanganate ($KMnO_4$) as an oxidizing agent mixed with deionized water (DI) and either sulfuric acid (H_2SO_4) or hydrofluoric acid (HF) are adopted as etchant. Nanoscale Au patterns were prepared by a soft lithography method. Fig. 1(a) illustrates the formation mechanism of GaAs NW arrays by MacEtch involving H_2SO_4 at high temperature of 40–45 °C. MacEtch begins when holes (h^+) are generated from the oxidant on the metal surface, and the holes are removed as soon as they reach the boundary of Au, GaAs, and solution. High aspect-ratio vertical GaAs NW array with diameter of ~600 nm were produced by this method, as shown in Fig. 1(b). Compare to the bottom–up approach, the top–down approach gives better control on the shape and dimension. The major challenges are the resolution limit of the diameters and the high facility cost. The top–down approach depends heavily on multistep lithography and lift-off techniques, which are expensive and time-consuming.

Bottom–up approach refers to the synthesis of NWs by employing their constituent atoms that grow anisotropically along the axial direction to obtain 1D single-crystalline structure. The 'vapor–liquid–solid' (VLS) method is a typical growth scheme that promotes seeding and oriented growth by introducing a catalytic liquid alloy phase, which can rapidly adsorb the vapor-phase precursor source to the supersaturation level, and then induce the precipitation of NWs and producing various types of semiconductor materials in a relatively large quantity[11, 12]. In details, during the VLS process, vapor-phase precursors are introduced at temperatures above the eutectic point of the metal-semiconductor system, resulting in liquid metal droplets. Continuously feeding the precursors leads to the supersaturation of catalytic droplets, upon which the semiconductor material starts to nucleate out of the melt and eventually grow into crystalline NWs. Another similar mechanism is known as the vapor–solid–solid (VSS) mode, whereby the catalyst remains in the solid phase during the

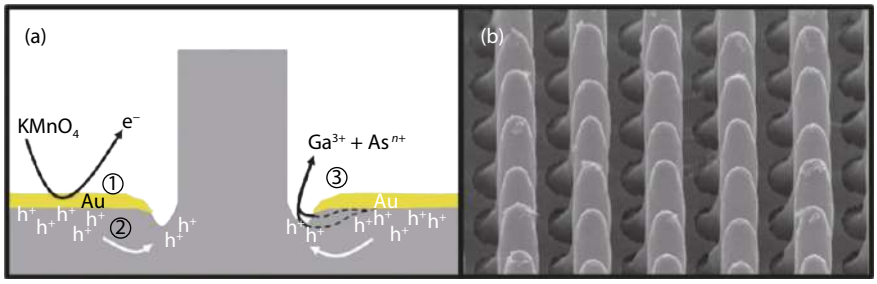

Fig. 1. (Color online) (a) Schematic illustrations of the formation mechanism of GaAs NWs. (b) SEM images of high aspect ratio GaAs NW produced from a 600 nm wide square Au mesh pattern in H_2SO_4 and $KMnO_4$ solution at 40–45 °C. Reprinted from Ref. [9] with permission, Copyright 2011, American Chemical Society.

NW growth. In this way, the particles can provide low-energy interfaces for trapping the precursor materials and yield higher epitaxial growth rates than elsewhere on the substrate[13]. Besides, other mechanisms such as the vapor-solid (VS) and oxide assisted growth (OAG) schemes do not require the existence of any catalyst, but the obtained NW diameter control becomes more challenging. As a result, the template-assisted (TA) mechanism as another common growth technique is introduced to achieve better NW diameter control by utilizing a prefabricated template, including anodic aluminum oxide (AAO) membranes and others in order to guide the NW growth. The NW diameter can be precisely manipulated by tuning the pore size of the AAO; however, an extra processing step is required to remove the template after the NW growth, increasing the risk of damaging the NW surfaces.

Among all these methods, the VLS mechanism is most widely used in the growth of NWs due to its simplicity and versatility. Various techniques have been adopted to generate vapor-phase precursors, for example, by decomposition of the semiconductor reactants in chemical vapor deposition (CVD)[14], or by energy transfer methods such as pulsed laser ablation[15] or molecular beam epitaxy (MBE)[16]. So far, CVD growth method has been widely explored in recent years for the growth of various NWs because of its relatively low setup and operating cost, simple growth procedures and, importantly, no involvement of toxic gas precursors compared to other sophisticated growth systems such as MBE and metal-organic CVD. In a CVD growth, metal nanoclusters serve as the catalysts and form liquid alloy seeds at a high temperature in a conventional tube furnace, and the solid powder source decomposes into gaseous precursors. Source powder is put at the upstream of a two-zone tube furnace, while hydrogen is used as a carrier gas to transport the evaporated source material to the downstream, and a substrate pre-coated with the metal catalyst is positioned at the downstream for the NW growth[17–19].

Solution-mediated wet-chemical approaches are widely used for NWs growth due to the relative simplicity and economical potential[20–22]. Micro/nanofluidic technologies can precisely manipulate not only fluid flows but also mass transport of small molecules at micro- and nanoscales, and potentially provide controllable and high-throughput parametric screening in wet chemical or solution-mediated fabrication processes[20, 23, 24]. Zhou *et al.* demonstrate a micro/nanofluidic fabrication method to produce methylammonium lead iodide ($MAPbI_3$) NWs in a controllable manner, which makes it possible to manipulate the initial nucleation point and subsequent growth path of perovskite NWs using $MAPbI_3$, as shown in Fig. 2. They use a micro/nanofluidic device with a crack-assisted nanochannel connected two microchannels and adopt the "crack-photolithography" to facilitate the production of polydimethylsiloxane (PDMS)-based micro/nanofluidic channel networks. The number of $MAPbI_3$·DMF NWs can be controlled by choosing the initial points and paths of PbI_2·DMF nanocrystal precursors when designing the micro/nanofluidic channel network, and the generation of PbI_2·DMF-related crystals is guided by the nanochannel and drives the growth of $MAPbI_3$·DMF NWs. The micro/nanofluidic fabrication technique enables precise control of the growth of $MAPbI_3$ NWs to manipulate the number, location, and orientation of the NW arrays. Flexible substrate materials can be used with the PDMS micro/nanofluidic platform for solution-mediated perovskite NW growth, indicating the potential of the micro/nanofluidic fabrication technique for low-cost, large-scale, flexible optoelectronic applications.

2.2. Assembly method for flexible electronics

In the previous section, some NW fabrication techniques is introduced. To integrate them into photodetector, special transfer and assembly method in a controllable manner is crucial especially for flexible devices. For single NW devices, the NWs are randomly distributed on substrate by drop-casting method. However, it's impossible to adopt this method with random and disordered NWs for large scale device arrays and mass production. For the fabrication of flexible NW detectors, typically there are two approaches: direct NW growth on flexible substrates and NW transfer to flexible substrates by different methods such as electrospinning method, contact printing, and peeling transfer method[25].

Recently, contact printing technique has attracted considerable attention, which can be utilized for large-scale assembly of NW parallel arrays on both rigid and mechanically flexible substrates followed by subsequent device fabrication. This approach can provide high performance and stable device operation at low cost[26–28]. A simple contact printing approach for wafer-scale assembly of highly ordered, dense and regular arrays of NWs with high uniformity and reproducibility were demonstrated by Fan *et al.*[28]. In this process, a growth substrate with dense NWs as the donor substrate is directionally slid on top of a receiver substrate coated with lithographically patterned resist, resulting in the direct transfer of aligned NWs to the receiver chip, as shown in Fig. 3(a). Lubricant can be used as a spacing layer between the two substrates to minimize the NW-NW friction during the sliding pro-

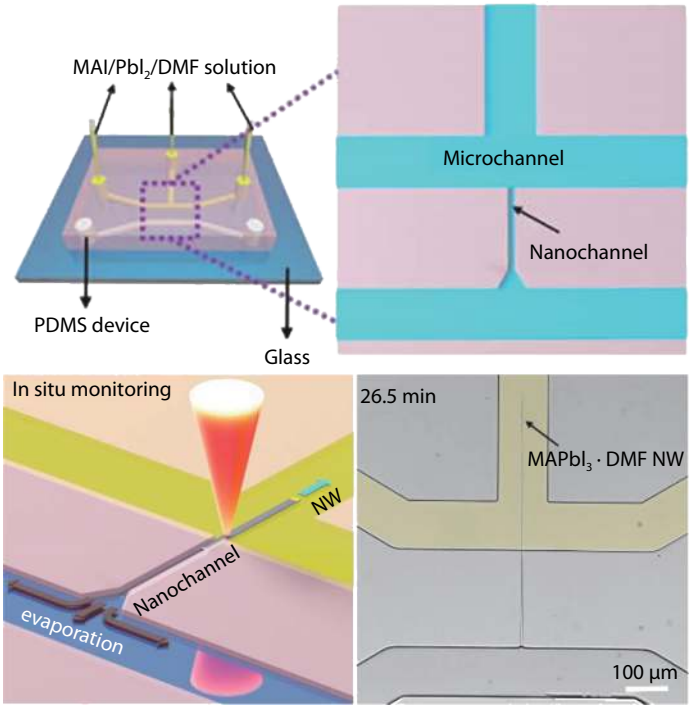

Fig. 2. (Color online) Illustration depicting the growth mechanism of a $MAPbI_3$·DMF NW by in situ monitoring with an UV–Vis microspectrometer. Reprinted from Ref. [20] with permission, Copyright 2018, American Chemical Society.

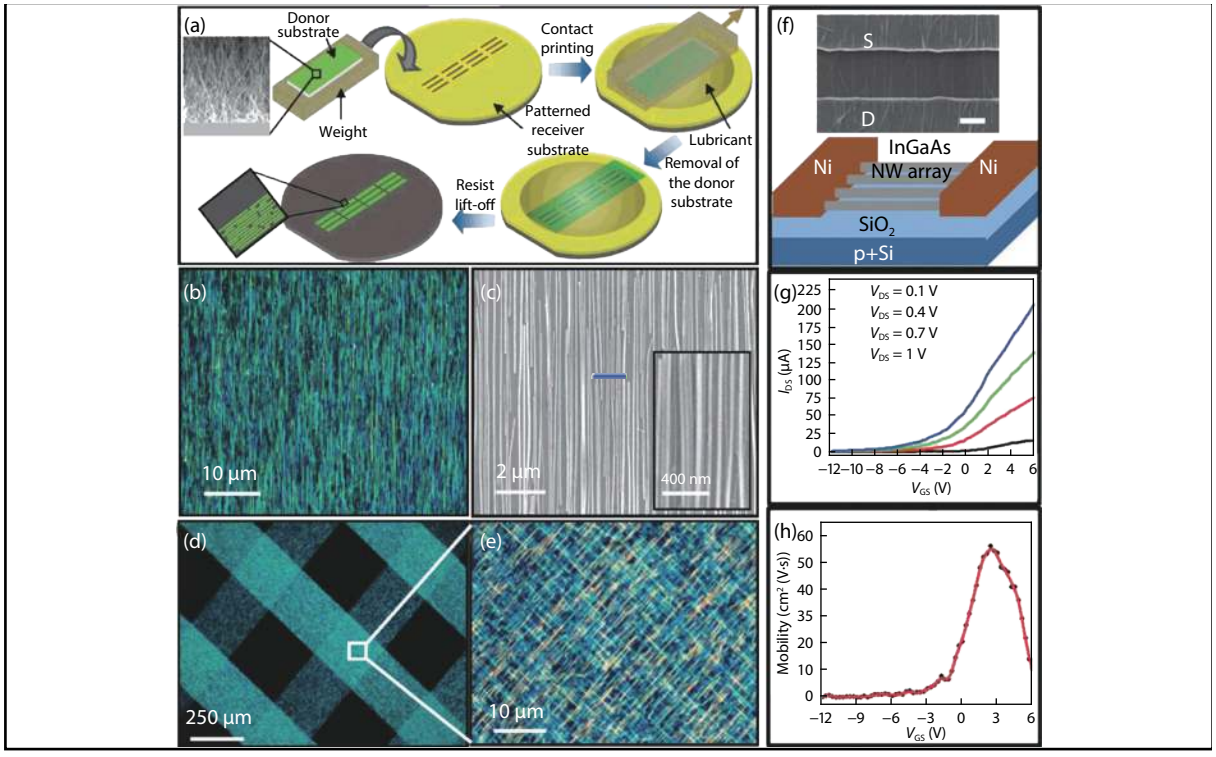

Fig. 3. (Color online) (a) Schematic of the process flow for contact printing of nanowire arrays. (b) Dark-field optical and (c) SEM images of Ge NWs (d ~ 30 nm) printed on a Si/SiO_2 substrate showing highly dense and aligned monolayer of nanowires. The self-limiting process limits the transfer of NWs to a single layer, without significant NW bundling. (d) and (e) Optical images of double layer printing for Si NW (d ~ 30 nm) cross assembly. Reprinted from Ref. [28] with permission, Copyright 2008, American Chemical Society; (f) (Top) SEM and (bottom) schematic of a back-gated InGaAs NW array FET. The scale bar is 1 μm. (g) Transfer characteristic of a representative InGaAs NW parallel device under V_{DS} = 0.1, 0.4, 0.7, and 1 V, about 200 NWs bridging S/D. (h) Mobility assessment of this NW array device under V_{DS} = 0.1 V. Reproduced from Ref. [29] with permission, Copyright 2012, American Chemical Society.

cess, and the density of the printed NWs can be easily modulated to meet the requirements of various NW-based device applications. After the NWs printing, the patterned resist was removed by a standard lift-off process, and the NWs were dir-

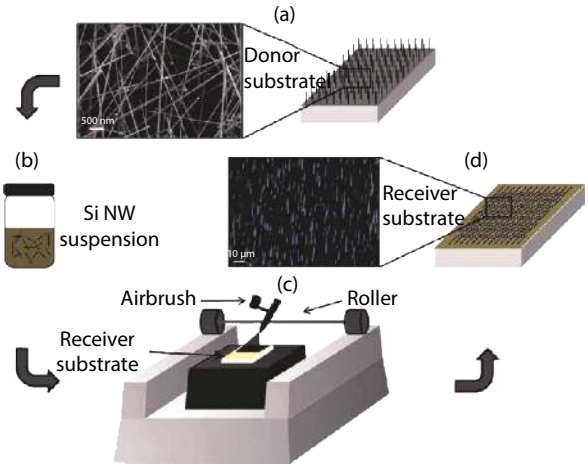

Fig. 4. (Color online) Schematic of the spray-coating process that involves a direct transfer of NW suspension to the receiver substrates. (a) Schematic and scanning electron microscopy (SEM) image of the NW sample used in this study. (b) Schematic of the NW suspension. (c) Schematic of the assembled apparatus used in this study. (d) Schematic and optical microscopy image of Si NW spray-coated on the SiO_x/Si substrate. Reprinted from Ref. [31] with permission, Copyright 2012, American Chemical Society.

ectly transferred from the growth substrate to the patterned regions of the substrate as parallel arrays. Figs. 3(b) and 3(c) present the optical and SEM images of assembled Ge NWs on the receiver substrate, demonstrating that the transferred NWs can form a uniform and well-aligned monolayer. Also, double layer printing of Si NW crosses can be achieved by a multi-step printing method as illustrated in Figs. 3(d) and 3(e), and the controlled stacking of NW crosses indicates the versatility of the contact printing method for optoelectronic applications.

As expected, the contact printing process can also be widely adopted for various semiconductor NWs, such as InAs, InGaAs and InGaSb NWs[26, 29, 30]. Hou *et al.* demonstrated the feasibility of large-scale integration of the NWs for electronic applications, and fabricated InGaAs NW parallel arrays by this contact printing method[29]. The SEM image and schematic of the printed NW array FET device are shown in Fig. 3(f), and the electrical transfer characteristics of a printed array with ~200 nanowires in the channel are shown in Fig. 3(g). The current density of this device is found to be ~1 μA/μm under V_{DS} = 1 V and V_{GS} = 6 V with an I_{ON}/I_{OFF} ratio of ~500, and the corresponding field-effect mobility against gate voltage, V_{GS}, is evaluated as shown in Fig. 3(h). The NW device performance can be further improved by the enhancement of the NW print density, the alignment, the channel length scaling, and the passivation of the NW surfaces. Furthermore, Takahashi *et al.* demonstrate GHz device operation of InAs NW arrays assembled on a mechanically flexible substrate for the first time[26]. The NW array transistors exhibit a maximum oscillation frequency of ~ 1.8 GHz, and a cutoff frequency of ~1 GHz which is due to the high saturation velocity of electrons in the high-mobility InAs NWs, confirming the potential of NW array FET devices for future high-performance electronic device and sensor applications. Besides, InGaSb NW parallel array photodetector with efficient photoresponse characteristics in the 1550 nm regime has been achieved by contact printing technique[30]. Ultrafast response times, ranging between 30 and 50 μs, has been observed for these NW parallel array devices.

Spray coating technique is a simple method for the deposition of highly ordered and aligned NW arrays on different substrates, including silicon, glass, metals, and flexible plastics with controlled density[31–33]. Assad *et al.* report an efficient spray-coating route for the deposition of highly ordered and highly aligned NW arrays on a wide range of receiver substrates as shown in Fig. 4[31]. The spray coating system consists of a hot plate for controlling the temperature of the receiver substrate, a pressure flow spray nozzle module, a nozzle movement module, a nozzle angle control module, and a nozzle cross-section control module. Well-aligned and well-controlled Si NW, GaN NW, and Ag NW arrays can be achieved under controlled conditions of the nozzle flow rate, droplet size of the sprayed NWs suspension, spray-coating angle, and temperature of the receiver substrate.

Electrospinning is a facile, cheap and efficient technology to fabricate randomly oriented NWs on certain substrates. During the electrospinning process, the precursor liquid forms a Taylor cone at first and then turns into a charged jet under high electrostatic voltage. The charged jet will be further elongated and thinned under electrostatic force and Coulomb repulsion during travelling from outlet of injector to collector. With simple modification, such as field assisted method[34–36], rotating collector assisted method[37–39] and near-field assisted method, highly ordered NW arrays can be achieved on various substrates with high throughput by electrospinning as well[40–45]. Liu *et al.* demonstrates an all-printable fabrication of parallel arrayed ZnO granular NWs (GNWs), which combines high throughput electrospinning and ink-jet printing[44]. Fig. 5 illustrates the schematic of the GNW printing system. Zinc acetate (ZnAc) is mixed in PVA (polyvinyl alcohol) as the solution for electrospinning, and the continuous electrospinning of ZnAc/PVA composite nanofibers occurred with 2 kV direct-current bias between the needle and the substrate to establish stable electrospinning. Based on this method, all-printable polycrystalline ZnO GNW photodetectors are achieved on flexible substrate, and this cost-effective fabrication process can be used for scalable fabrication of high-performance flexible electronic and optoelectronic devices.

Most transfer methods make NWs positioned horizontally on the substrate and the initial NW orientation cannot be maintained. Recently, an alternative transfer method yielding vertical NWs has gained a broad interest, which is based on NW embedding in a polymer layer followed by mechanical peeling of the membrane[25, 46]. Zhang *et al.* employ a mechanical peeling transfer method as shown in Fig. 6 to transfer a composite NW/polymer membrane onto a flexible substrate, and demonstrated a flexible nitride p–n photodiode[25]. The NWs are embedded into a polymer layer and the polymer/NW membrane is mechanically peeled-off, contacted and mounted on a piece of a copper tape. The lift-off and transfer procedure enables the assembly of free-standing layers of NW materials with different bandgaps without any constraint related to lattice-matching or growth conditions compatibility[46]. A fully flexible transparent contact based on a silver NW network is used, which allows bending the detector to a few millimeters curvature radius without damage. This method allows for a large design freedom and modularity

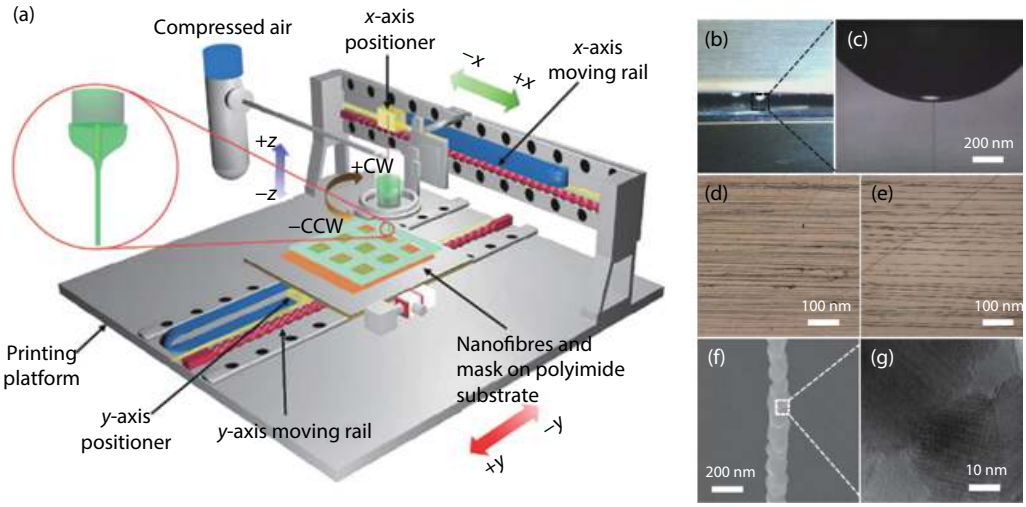

Fig. 5. (Color online) Schematic of two-step all-printable process and materials characterization. (a) Printing setup schematic. (b, c) Electrospinning ejection from the tailored cone apex. (d, e) Optical images of the as-printed electrospun ZnAc/PVA nanofibres with 5 and 10 mm spacing, respectively. (f) SEM image of an as-calcinated ZnO GNW. (g) Transmission electron microscopy image of a GNW. Reprinted from Ref. [44] with permission, Copyright 2014, Springer Nature.

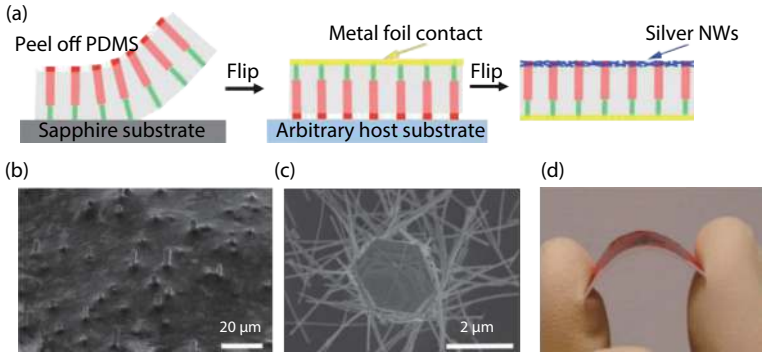

Fig. 6. (Color online) (a) Schematic representation of the fabrication steps: encapsulation in PDMS and peel-off of the membrane; deposition of the back metal contact; deposition of the top transparent contact composed of a silver nanowire mesh. (b) Bird's eye view SEM image of the top surface of the detector. (c) Top view SEM image of an individual nitride NW contacted with silver nanowires. (d) Device photo illustrating its flexibility. Reproduced from Ref. [25] with permission, Copyright ©2016, American Chemical Society.

since it enables combination of materials with very different physical and chemical properties, which cannot be achieved by monolithic growth.

3. Nanowire-based flexible photodetector

Based on the optoelectrical properties, there are different group of 1D nanostructures that are capable to be integrated into photodetector. In this section, the recent development of NW-based flexible photodetectors is reviewed based on different material groups.

3.1. Group IV materials

3.1.1. Carbon nanotube

Carbon nanotube (CNT) is one of many allotropes of carbon, which is an interesting family that have intriguing optoelectronic properties depends on their molecular dimensionality[47]. Depends on the chirality of the CNT, it can be categorized as either metallic or semiconducting. Both metallic and semiconducting CNT can generate photocurrent upon the illumination, which originates from two different mechanisms[48]. There are several intriguing properties that make CNT an attractive material for flexible photodetector. First of all, the exciton lifetime of a semiconducting CNT is up to ns range[49]. Combining with high carrier mobility, CNT is one of the most intriguing candidates for high performance flexible photodetector. Also, the superposition of a CNT film can be tuned by blending CNT with different chiralities. Therefore, the absorption of the CNT film can be tuned from visible light (Vis) to infrared (IR) to THz range[47]. The applicability by spray coating and printing of CNT film is also important for applying the CNT on flexible substrate in low cost and high throughput manner[50]. A fully printable flexible CNT photodetector was fabricated by Zhang *et al.*[51]. Apart from the CNT ink, all the electrodes (source, drain and gate) and the gate dielectric layer are consisted of printable ink. The results demonstrate that by using the ink of different materials, a fully printable flexible photodetector can be constructed.

In recent years, lots of research input is focus on the IR sensing based on CNT-based flexible photodetector. One of many motivations of developing CNT-based IR detector is the possibility of working in room temperature. Traditionally, IR-detector based on InGaAs and HgCdTe shows very good performance. However, those good performance can only be achieved when they are sufficiently cooled[52]. CNTs provide

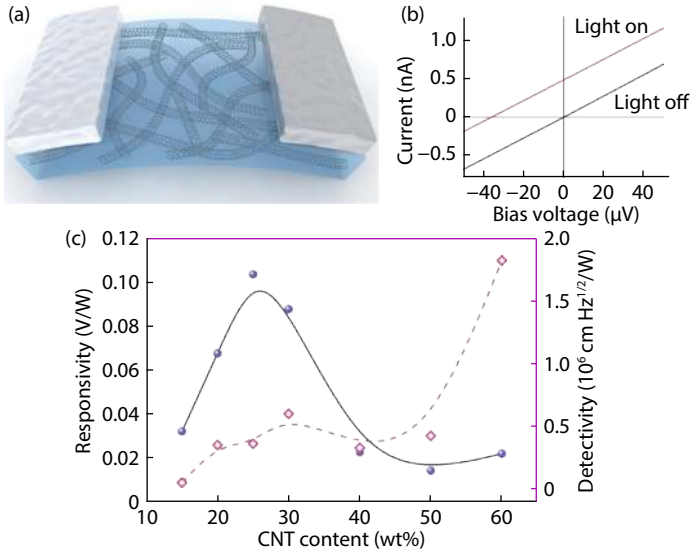

Fig. 7. (Color online) (a) Scheme of the PVA/CNT flexible photodetector. (b) *I–V* characteristic of the photodetector with and without 523 K blackbody illumination in 25 wt% CNT device. (c) Responsivity and detectivity trends according to the CNT content wt%. Reproduced from Ref. [4] with permission, Copyright 2018, American Chemical Society.

an alternative for room-temperature IR sensing. Liu *et al.* demonstrated a CNT-based broadband IR detector that have photoresponse from 785 to 2100 nm on SiO_2/Si substrate[53]. For flexible CNT-based IR sensor, a p–n junction of multi-walled CNT-based photodetector has demonstrated to be capable of sensing IR signals with low power density at room temperature[54]. Apart from IR sensing, CNT can also be integrated into flexible visible light sensor[51, 55], X-ray image sensor[55] and wearable terahertz scanner[56].

Although pure CNTs film can be used as the sensing materials, to further improve the photodetector performance, CNT-based heterostructures are also frequently studied. For example, CNT/other carbon allotropes based heterostructures can enhance the IR sensing. In a research of Park *et al.*, fullerene (C_{60}) was deposited on a bilayer of semiconducting single-walled CNT (sc-SWCNT)[34]. The SWCNT/C_{60} phototransistor showed an improved responsivity, photoconductive gain, and specific detectivity. The improved device performance is because of photoinduced electrons trapping enabled by the existence of C_{60}. The carrier recombination time is hence increased[35, 36]. Another frequently studied CNT-based heterostructure is graphene/CNT heterostructure. Although graphene has many intriguing optoelectrical properties, the photoresponsivity of graphene photodetector is limited (~10^{-2} A/W) in earlier studies due to the inefficient light absorption of single layer graphene[37, 38]. Broadband photodetector based on graphene/CNT hybrid film was constructed on rigid surface (SiO_2/Si) by Liu *et al.*[39]. The photodetector exhibits a high photoconductive gain, high electrical bandwidth across Vis to IR range (400–1550 nm). It also shows a high photoresponsivity (> 100 A/W) and a fast response time (about 100 μs). The improvement compared to other graphene photodetector can be attributed to the atomically flat graphene that reduces the number of trap density on the surface. Also, the built-in potential between the interfaces enhance the effective separation of the electron-hole pair and reduce the recombination rate. Also using the graphene/CNT hybrid film, Liu *et al.* fabricated a flexible photodetector on PET substrate[57]. The photodetector demonstrated high photoresponsivity (about 51 A/W) and fast response time (about 40 ms) over visible range. It is worth mentioning that not only the device performance is enhanced in these all carbon based photodetector when the bending is absent, the devices also performed well under bending which demonstrated the mechanical robustness of the CNT/carbon allotropes heterostructure[34, 57].

Another frequently studied CNT hybrid system is CNT/polymer system. On rigid sample, polymer like electrically and thermally insulating polycarbonate[58], semiconducting polymer like poly(3-hexylthiophene- 2,5-diyl) (P3HT)[59] were studied. These CNT/polymer composites improve the photodetection performance by enhancing the exciton separation at the CNT/polymer[58, 59] and reduce the recombination rate by separating the CNT[58]. For flexible CNT/polymer-based photodetector, for example, Zhang *et al.* developed a poly(vinyl alcohol) (PVA) and carbon nanotube (CNT) composite-based self-powered thermal detector for body thermal imaging (Figs. 7(a) and 7(b))[4]. The thermal detector is based on the photo-thermoelectric (PTE) effect of the PVA/CNT composite. The advantages of using PVA to warp around the CNT is to enhance the PTE performance[60], the compactness and the biocompatibility. The weight percentage of the CNT in the composite is found to impact the detectivity of the detector due to the improvement in photon absorption and thermoelectric conversion efficiency with increasing CNT wt% up to 60 wt% (Fig. 7(c)). With optimization, the best reported detectivity of the thermal imaging device is up to 4.9×10^6 cm $Hz^{1/2}$ W^{-1}[4].

It is worth mentioning that, despite this review mainly focus on the 1D nanostructure as the sensing material in the photodetector, conductive CNT film-based electrode is also being developed for optoelectronic devices due to its mechanical flexibility and the transparency[61, 62].

3.1.2. Silicon nanowires

The advancement of the morden technology is mainly due to the development of silicon processing technology. Silic-

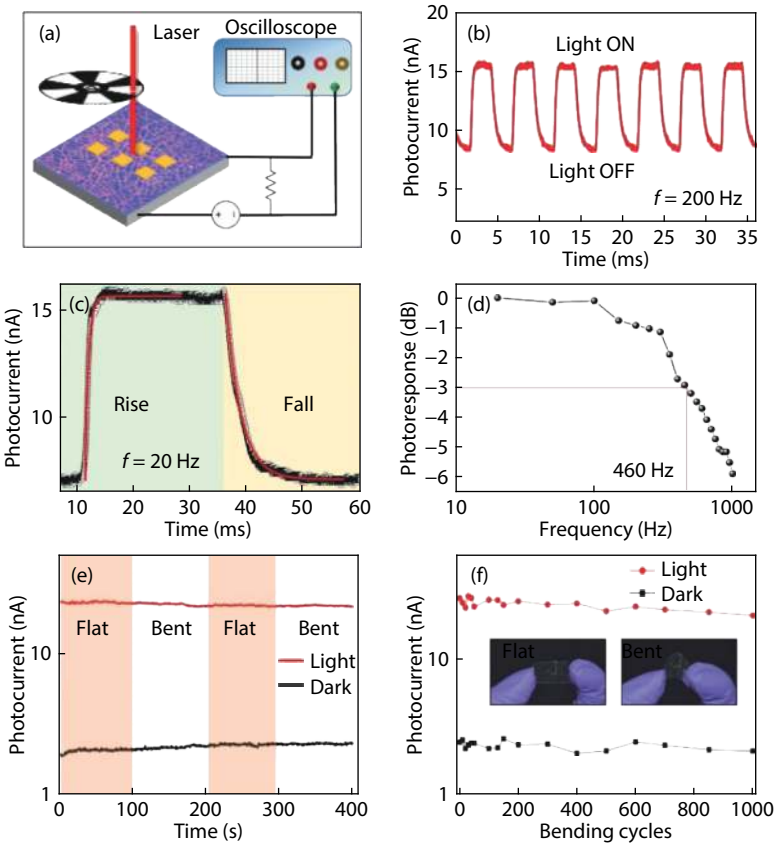

Fig. 8. (Color online) (a) Schematic of the measurement setup of the flexible percolative Si NW photodetector; (b) The transient photocurrent of the photocurrent. (c) The rise time and decay time, (d) the photoresponse at different frequency, (e) time-dependent photocurrent and dark current when the photodetector is bent or flat, and (f) the photocurrent and dark current of the flexible percolative Si NW photodetector as a function of bending cycles. Reproduced from Ref. [67] with permission, Copyright 2018, American Chemical Society.

on has been extensively used in computer chip, solar cell and sensors. While being one of the most abundant elements on earth, which make it more affordable, easy to dope and forming stable oxide are the main reasons why silicon is widely used in microelectronic industry. Traditionally, silicon is rigid and bulk which is not usable for wearable and foldable electronics. Creating the nanostructures of silicon changes mechanical properties drastically and enhance its flexibility, which allows it to be integrated into wearable and foldable electronics[63].

The NW form of silicon is studied for photodetector applications. As the maturity of silicon NW fabrication from both top-down and bottom-up approaches, the assembly of Si NW on flexible substrate can be done by different methods. For example, large scale of Si NWs can be fabricated by a cost-effective MacEtch method on a silicon substrate[64]. Follow by sonication and vacuum filtration, the Si NWs can be collected on filtration membrane and ready for transfer to a flexible substrate by the stamping process[65]. Using this approach, Huang *et al.* fabricated a Si NW network/Ag NW network photodetector on PET substrate which showed a fast dynamic response, partial transparency and good flexibility. Also, using the MacEtch, Kim *et al.* fabricate porous Si NW for flexible photodetector integration[66]. The NWs were aligned between the electrodes by applying an electric field between the electrodes. With the hydrazine passivation on the Si NW surface, the photodetector shows rapid response up on the illumination of red, blue and green light.

Recently, Hossain *et al.* integrated the a single-crystalline percolative Si NW to a transparent and flexible photodetector (Fig. 8(a))[67]. The NW network structure provides high transparency (~92% at 550 nm) on PET substrate. The photodetector based on the Si NW network showed broadband detection (350 to 950 nm). It also showed good responsivity, fast response time (Figs. 8(b)–8(d)) as well as good durability under multiple mechanical bending (Figs. 8(e)–8(f)).

3.2. III–V nanowires

With the excellent electrical and optoelectrical properties, III–V NWs are the ideal candidates for next-generation electronics and optoelectronics[68]. Compare to other 1D nanomaterials, III–V NWs demonstrated higher carrier mobility and higher intrinsic carrier concentration. Another important property of III–V materials is their direct bandgap which is important to be considered for high performance optoelectronics integration. High performance III–V NW has been demonstrated by various group. For example, Miao *et al.* demonstrated the first room temperature InAs NW IR photodetector[69]. The photodetector shows a board sensing range (from 632 nm to 1.5 μm). The Schottky–Ohmic contacted photodetectors shows a high photodetectivity and good stability. Recently, a board band ultrafast InGaSb NW photodetector which the response time is under 40 μs for Vis and NIR sensing[30]. High quality III–V NW has also been studied for flexible solar cell[70]. Despite of the high performance device demonstration, on the other hand, high quality III–V NWs are

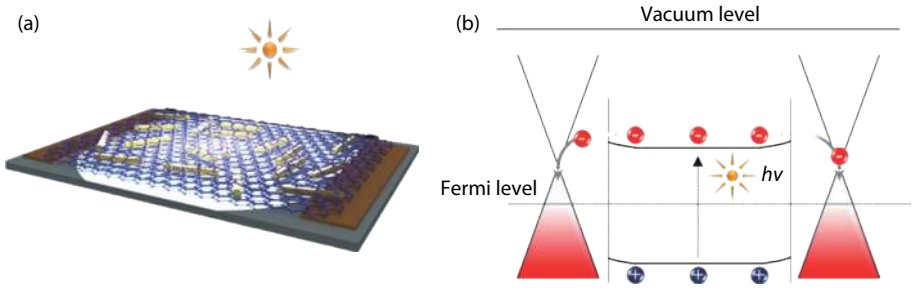

Fig. 9. (Color online) (a) Schematic and (b) the band diagram of the transfer process of the GaN NW/graphene sandwich photodetector. Reproduced from Ref. [75] with permission, Copyright 2018, American Chemical Society.

usually grown in high-temperature process which is not compatible with the flexible substrate[29, 71]. Especially, up to the knowledge of the authors, there is no reported method to grow vertical III-V NW array on flexible substrate like paper and polymer substrate which is frequently used to fabricate flexible photodetector. Therefore, special transferred techniques are necessary to be developed. That might be one of the reasons why the III–V NW based flexible photodetector are less developed.

Single III–V NWs were explored for flexible photodetector integration[72, 73]. High performance single GaSb NW photodetectors were fabricated on both rigid (SiO_2/Si) and flexible polyethylene terephthalate (PET) by Luo *et al.*[73]. Comparing the performance of these two substrates, the responsivity and external quantum efficiency of the flexible device dropped (from 7350 to 3690 A/W and (from 26000 to 13098, respectively) but remained admirable under the illumination of 350 nm light. One the other hand, the detectivity is increased by two times. The electrical stability of the GaSb NW photodetector was also demonstrated and the stability was good under different curvature and after certain bending cycles.

Some special device structures have been demonstrated on flexible GaN NW photodetector. For example, Zhang *et al.* demonstrated to integrate the vertical GaN/InGaN NW array on a polymer membrane for UVA detection[25]. The vertical NW array consisted of some core/multishell p–n junction GaN/InGaN NWs. This complex NW heterostructure would be beneficial for photodetector applications and attracts a lot of attention recently[74]. Using the mechanical peeling transfer method mentioning in the assembly section, the GaN/InGaN NW arrays were transferred on PDMS substrate[25]. After applying Ag NW network as the top electrode, the device structure shows good flexibility that the bending radius can be up to few millimeters without damaging the device. The peak responsivity was 0.0096 A/W under 370 nm illumination under zero bias. The low responsivity is possibly due to low NW density. On the other hand, the photodetector shows fast operation speed. Another special device structure is demonstrated by Han *et al.* Sandwiched by two graphene layers[75], GaN NW-based photodetector was fabricated. In their demonstration, the GaN NWs were transferred on top of a graphene layer and covered by another graphene layer (Figs. 9(a) and 9(b)). The sandwich structured photodetector shows a high photoresponsivity compared to other reports. The good device performance can be attributed to the enlarged effective interface between GaN NWs and graphene. Further improvement is expected by increasing the NW density. The device has good mechanical stability that after 200 bending cycles, the photoresponsivity remained at 97.1%.

Overall, the research input for III–V NWs as the sensing materials for flexible photodetector is still in infancy and the existing reports mainly focus on nitride-based or phosphorus-based III–V materials, which are mainly for UV–Vis photodetection. In group III–V family, III–As and III–Sb usually has small bandgap that can be used for short-wave IR (1–2.5 μm), mid-wave IR (3–5 μm) to long-wave IR (8–12 μm) sensing[76]. Flexible III–V NW IR detector that work in these regions is not yet demonstrated. Therefore, as an important material group for IR sensing, more effort is expected to be invested in III–V NW-based flexible photodetector, especially on III–As and III–Sb NWs.

3.3. Metal oxide nanowires

Metal oxide is one of the most studied materials for various applications, from sensing to electronic component, to heavy metal ions filtering[77–80]. As the metal oxides usually process wide bandgap, they are frequently integrated into UV or Vis sensor. Frequently studied metal oxide NW includes binary oxide, like ZnO[38, 81] and Ga_2O_3[82], as well as ternary oxide, like Zn_2GeO_4 and $In_2Ge_2O_7$[83]. Flexible UV sensors based on these oxide materials are also studied with various low cost fabrication methods. Take ZnO NWs, one of the most studied metal oxides, as an example, ZnO has a large bandgap (3.37 eV) and large exciton binding energy (60 meV) which means it is useful for UV detection. On rigid substrate, ZnO-based photodetector has demonstrated high responsivity (10^5 A/W)[84], high photoconductive gain (10^6)[84] and high detectivity (2.32×10^3%)[85]. The performance can be greatly improved by some surface modification or integrated with other materials like graphene[86, 87]. It can be directly fabricated on various flexible substrate like polymer substrate[88–90] and paper substrate[91]. All these examples highlight the potential of metal-oxide based NWs for high-performance flexible photodetector integration.

Despite remarkable progress has been achieved, the NW photodetector constructed by homojunction NW as the sensing materials have a lot of setback compares to their heterostructure counterpart. Recently, more efforts are put into fabricating metal oxide NW heterostructures. Here on, some recent examples about flexible photodetector based on metal oxide NWs-based heterostructures are introduced.

Surface decorating the surface of metal oxide NWs with QDs is one approach to enhance the device performance. For example, decorating the Zn_2SnO_4 NWs with ZnO QDs can enhance photocurrent and responsivity[92]. Shen *et al.* also used

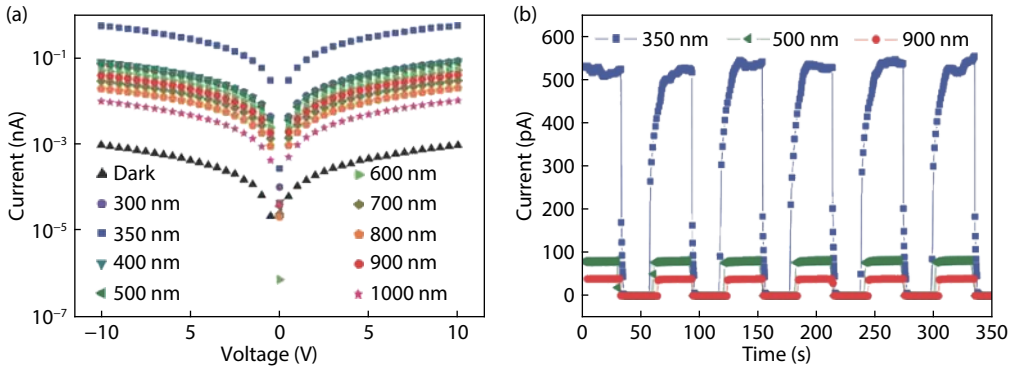

Fig. 10. (Color online) (a) *I–V* characteristic of the ZnO NW array/ PbS QDs photodetector under the illumination of different wavelength. (b) Transient response of the photodetector under different wavelength. Reproduced from Ref. [81] Copyright 2017 The Authors. Published by WILEY-VCH Verlag GmbH & Co. KGaA, Weinheim.

graphitic carbon nitride QDs to enhanced the performance of a flexible ZnO NW photodetector[93]. On the other hand, combining the metal oxide NWs with small bandgap materials is an effective way to expand the sensing region from UV–Vis to NIR range. ZnO NWs are usually used for UV photodetector integration. With the surface decoration of PbS QDs, the sensitive spectral range of ZnO NWs is broadened as PbS QDs has a narrowed bandgap and can be used for NIR sensing. The technique can also be used on flexible photodetector. Zheng *et al.* fabricated a ZnO NW array/ PbS QDs film for a UV–Vis–NIR photodetector[81]. The ZnO NWs array was fabricated by electrospinning and calcination technique on mica substrate. The PbS QDs were then attached on the NW array by a repeated spin-coating process and followed with a ligand exchange process to replace the long ligand with shorter ones to enhance the charge transfer between the NWs and QDs. This system broadens the sensing region of the flexible photodetector (Figs. 10(a) and 10(b)) and it remains stable after 200 cycles of 180° bending which is important when fabricating flexible metal oxide-based board band photodetector[81]. The small bandgap QD decoration technique was also demonstrated on SnS QDs/ Zn_2SnO_4 NW for flexible broadband photodetector[94].

Recently, metal oxide NW photodetector integrated on fiber-like substrates attracts some research interest for the application in smart textile[95–99]. The NWs can be transferred or directly grown on fiber substrate like metal wire[95, 96], KEVLAR wire[98] and carbon fiber[98]. Apart from the flexibility and knittability, another advantage of this type of photodetector is the capability of omnidirectional photosensing. Also, by careful material selection, self-powered photodetector can be constructed. Dong *et al.* constructed a self-powered fiber-shaped photodetector based on ZnO NW/PVK layer[95]. The photodetector shows photoresponse under the illumination of UV light, but the performance was not satisfying. Recently, Sun *et al.* fabricated a fibrous self-powered broadband photodetector by connecting a perovskite-TiO_2-coated carbon fiber and a CuO NW-CuO coated Cu wire[99]. The photodetector demonstrated a high detectivity (2.15×10^{13}) under the illumination of 800 nm light without bias. The dark current was suppressed to 10^{-11} A by the electron blocking layer and the photodetector also has a stable response time (200 ms) after tens of 90° bending cycles.

3.4. Metal chalcogenide nanowires

Chalcogenide NW is a group of NWs that contain S, Se or Te as their anions. Some of these materials have direct bandgap and as their bandgap lie in the visible light region which makes them potential candidate for optoelectronic that works in Vis region. Metal chalcogenide materials include some II–VI semiconductors (like CdS and SnS) and materials like Sb_2S_3 and In_2S_3. Their NW form are frequently used to be integrated into rigid substrate-based photodetector[100, 101]. Considering the large materials family, the integration of chalcogenide NW into flexible photodetector is rare in recent years.

Cadmium based II–VI NW like CdS and CdSe NWs were integrated into flexible photodetector. Branched CdS NWs were fabricated by Li *et al.* which exhibit high detectivity on rigid substrate[102]. When integrated into the flexible photodetector, the device performance is comparable to the rigid counterpart and also demonstrated good flexibility, electrical stability and good endurance against folding[102].

Recently, the III–VI NWs have shown some promising result for flexible photodetector integration. Single crystalline In_2S_3 NWs have demonstrated a high on-off ratio (10^6)[100]. The photodetector also exhibits high sensitivity and quantum efficiency[100]. Sb_2S_3 is another interesting material due to its stability and have a narrow bandgap (1.21 eV). Its NW-based flexible photodetector was also studied using different NW synthesis method and showed good flexibility and stability[103, 104].

3.5. Perovskite nanowires

Hybrid organic-inorganic are recently attracting tremendous amount of research interest for solar cell and photodetector[35, 105–107] due to their exceptional optical and electrical properties. For example, this type of material has direct bandgap, board absorption range (from UV–Vis to NIR), high light absorption coefficient, long carrier lifetime and diffusion length and high carrier mobility[108]. Also, the low-temperature fabrication process makes them capable to be directly fabricated on flexible substrate like PI and PET. The low production cost is another advantage.

The stability of perovskite material against the surrounding environment has been a concern. For flexibility photodetector, as it would under bending and continuous bending cycles, the stability issues become more important to be con-

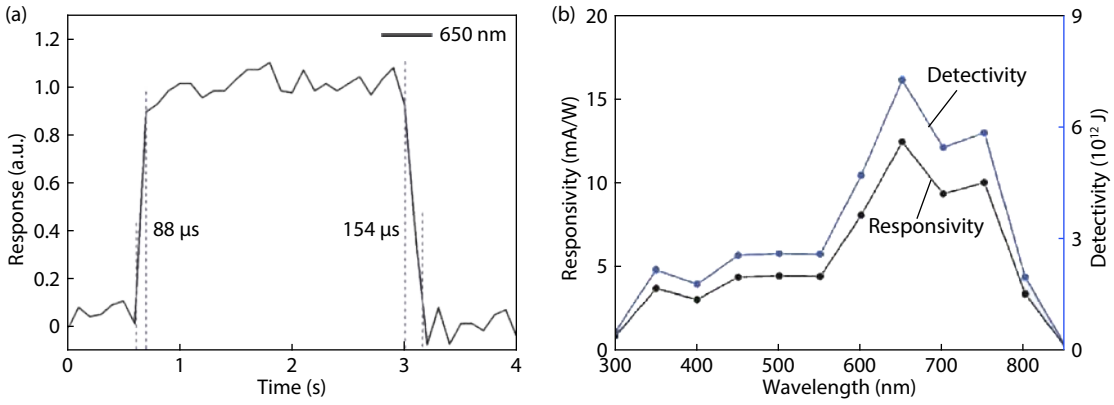

Fig. 11. (Color online) (a) The rise time and decay time and (b) the responsivity and detectivity curves of the perovskite NW photodetector at 0 V. Reprinted from Ref. [112] with permission, Copyright 2019, WILEY-VCH Verlag GmbH & Co.

sidered. There are various reports focusing on how to improve the stability of the organic–inorganic perovskite NW on flexible photodetector. For example, single-crystalline $CH_3NH_3PbI_3$ NWs based photodetector can remain stable after 45 days of storage due to the high crystal quality of the NW produced by the saturated vapor-assisted crystallization method[109]. As the NW can be used for flexible photodetector, it's also important to improve the stability of them on flexible substrate. Using a low-temperature solution-based process, Auso *et al.* fabricated a thiocyanate-doped $CH_3NH_3PbI_{3-x}(SCN)_x$ perovskite NW network on Kapton substrate[110]. Despite of the low-temperature process, the addition of pseudohalide, SCN^-, helps to improve the crystal quality and hence reduce the recombination losses and improves the photo absorption, charge generation and charge transport across the NW network and the electrodes. The NW network device is hole-dominant like and with a passivated coating of PMMA, the device performance is enhanced. After the PMMA coating, the dark current is reduced while the photocurrent is improved which indicated the PMMA blocked the oxygen and water molecules penetration into the perovskite that degrade the device performance. The device also shows high specific detectivity (7.3×10^{12} J) and with response time about 200 μs (227.2 μs for rise time and 215.4 μs for decay time) which are excellent performance among organometal halide perovskite flexible photodetector. The photocurrent remains 80% of its initial value after 15000 bending cycles and the morphology of the perovskite does not change much. Also, the PMMA-passivated devices lose less than 2% of their initial photocurrent after storing in ambient air for 30 days. In another report, using potassium ion assisted synthesis, the $(C_4H_9NH_3)_2PbBr_4$ nanobelt also demonstrated good stability after continuous bending and can be stored under ambient condition for 20 days with no phase degradation[111].

As the fabrication of perovskite can be done in low temperature, it can be directly fabricated on the flexible substrate without the need of transfer. Zhou *et al.* growing the perovskite NWs using micro/nanofluidic fabrication technique and integrated them into flexible photodetector.[20] Using a DMF-mediated crystallization method, the initial growth site and the growth path of the $MAPbI_3$ NWs can be guided by a micro/nano fluidic channel on flexible substrate. Deng *et al.* fabricated the $CH_3NH_3PbI_3$ microwires array on PET substrate using blade coating method. The microwires array fabricated by this method not only has good crystallinity but can also be stored over 50 days with only a mild fluctuation.

One recent report employed ferroelectric poly(vinylidene-fluoride-trifluoroethylene) (P(VDF-TrFE)) and hybrid perovskite NW to construct a flexible self-powered photodetector that is also semi-transparent[112]. After poling of the P(VDF-TrFE), an internal electric field is built-up and improve the photoinduced electron–hole pair separation. With the optimizing the treatment condition of the ferroelectric polymer, the flexible demonstrated a high detectivity at 7.3×10^{12} J and fast response time (rise time at 88 μs and decay time at 154 μs) (Figs. 11(a) and 11(b)). The mechanical properties of the hybrid perovskite NW/ P(VDF-TrFE) composite also have good mechanical stability.

Apart from the organic-inorganic perovskite NWs, pure inorganic NWs are also investigated for high performance photodetector due to the better stability[113]. One report integrated the pure inorganic NWs for flexible linearly polarized photodetectors[114].

4. System integration of NW-based flexible photodetector

So far, the recent developments of the NW-based flexible photodetector are reviewed. However, individual photodetector is not enough for imaging applications but to integrated large amount of photodetector into photosesning matrix. On the other hand, extra power source is always needed for photodetecting devices. To take the full advantage of the flexibility and compactness of the flexible photodetector, self-powered photodetector is also an important development. These two developments will pave the way for flexible photodetector integration for different applications.

4.1. Image sensor

Image sensing is an important application of photodetector. The ability of sensing different wavelength gives rise to their unique applications. Infar-red sensing, for example, can be used in medical analysis, process monitoring and control, night vision, security and etc.[115]. Visible light sensing is important in developing electronic eyes[116] and face recognition system. UV imaging can be used for forensic[117], skin condition monitoring[118], remote sensing[119], oil spill detecting[120] and electrical power line inspection[121]. Flexible image sensor provides even more interesting applications than

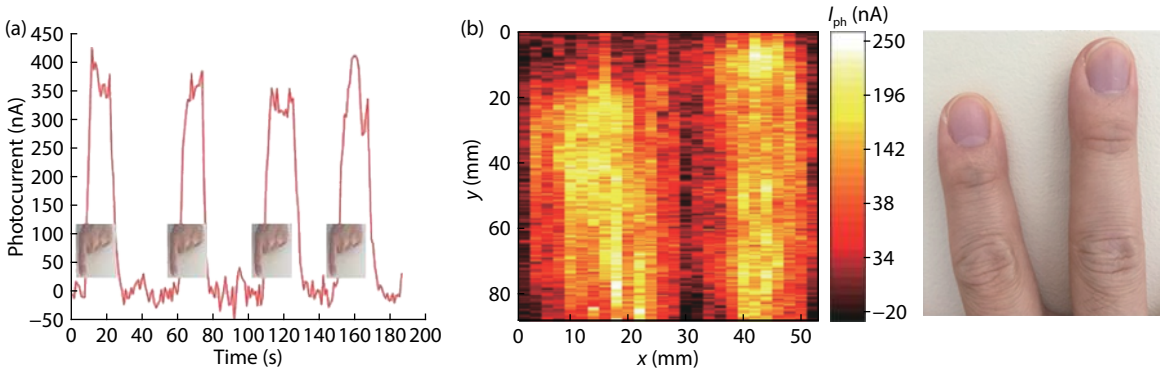

Fig. 12. (Color online) (a) Human fingertip radiation detection at different by the CNT/PVA image sensor. (b) (left) The thermal image of the human finger on the right. Reprinted from Ref. [4] with permission, Copyright 2018, American Chemical Society.

conventional rigid photodetector. For example, to monitor the real-time skin temperature distribution, the IR image sensor should be flexible enough to warp around and attach to the curved body part. Such sensor can provide information about the blood perfusion and be used for early breast cancer detection, brain imaging, rehabilitation monitoring and etc.[122]. The NW-based flexible photodetector has also been used to construct the image sensors in recent years.

As mentioned, CNT can be used for IR sensing. Zhang *et al.* developed a poly(vinyl alcohol) (PVA) and carbon nanotube (CNT) composite-based self-powered thermal detector for body thermal imaging[4]. The thermal detector is based on the photo-thermoelectric (PTE) effect of the PVA/CNT composite. The advantages of using PVA to warp around the CNT is to enhance the PTE performance[60], the compactness and the biocompatibility. The weight percentage of the CNT in the composite is found to impact the detectivity of the detector due to the improvement in photon absorption and thermoelectric conversion efficiency with increasing CNT wt% up to 60 wt%[4]. The authors also demonstrated a non-contact mode human body thermal imaging by holding the fingertips ~2 mm away from the surface (Fig. 12(a)). The margin of the fingertips can be clearly identified by the photodetector (Fig. 12(b)).

Li developed a flexible UV image sensors array based on ZnO QD decorated Zn_2SnO_4 NW heterojunction photodetector[92]. The photodetector exhibits ultrahigh light-to-dark current ratio (up to 6.8×10^4), specific detectivity (up to 9.0×10^{17} J), photoconductive gain (up to 1.1×10^7), fast response, and excellent stability. The QD on NW structure enhances the photocurrent and responsivity (~10 times) originates from the energy band engineering, which improve the electron-hole pairs separation at the QD-NW interface. When the photodetectors are integrated into a 10×10 device array, the clear image of letters "F" and "E" can be clearly displayed under different bending conditions.

Several groups developed image sensor that work in visible light region. Flexible image sensor based on 3D perovskite NW array was built by Gu *et al.*[123]. Using a free-standing porous alumina membrane as a guiding template, the $MaPbI_3$ NW array was grown in a two-zone furnace using Pb and methylamine iodide as precursor source. The grown NWs have good crystallinity and uniform in size. One advantage of this type of NW array is the antireflection and light-trapping effect, which ensure a better light absorption than conventional planner semiconductor sample[124]. A 1024 pixel image sensor was built based on the 3D NW array on PDMS. The authors demonstrated the real-time image capturing ability by moving the light-spot (source) on the image sensor and capture the movement. Another perovskite microwire (MW) array-based image sensor was constructed by Deng *et al.*[125]. The fabricated MWs have good optoelectronic properties and stability. When fabricating the MWs on PET substrate, the image sensor shows high performance for high-resolution image sensor. Another demonstration of image sensor is done by Li *et al.*[94]. Using SnS QD/Zn_2SnO_4 NW structure, a 10×10 array flexible broadband image sensor was constructed, which is capable to sense the white light and red light even under bending condition. Those are important demonstrations that high performance image sensor can be built by 1D NW structures.

Turning electrical signals into images is more complicated than just building a photodetector. The construction of individual NW array photodetector unit and the design of the electrodes is complicated. The size of the individual NW array and the electrodes affect the overall resolution of the image sensor. Also, the spacing between these individual units also limits how many pixels can be built on the substrate. The existing reports usually contain larger pixels and wide spacing. For real-life application, smaller pixel size and narrower spacing is necessary which will challenge some current assembly techniques

4.2. Self-powered photodetectors

Another development of NW based flexible photodetector toward practical application are developing self-powered photodetector or self-powered photosensing unit[126]. The purpose of such development is to reduce the overall weight of the whole sensing system. A sensing unit usually constructed by a light sensing unit, an electrical signal measurement unit and a power unit. Integrating an external power unit increases the extra weight to the whole system. Eliminating the external power unit or replace the traditional rigid power source to flexible one will benefit to some applications like wireless health monitoring or soft robot development. That can be done by two approaches. One is creating a built-in potential difference across the photodetector unit and the other one is integrating flexible power source within the same unit[5].

Building a built-in potential difference can be done by

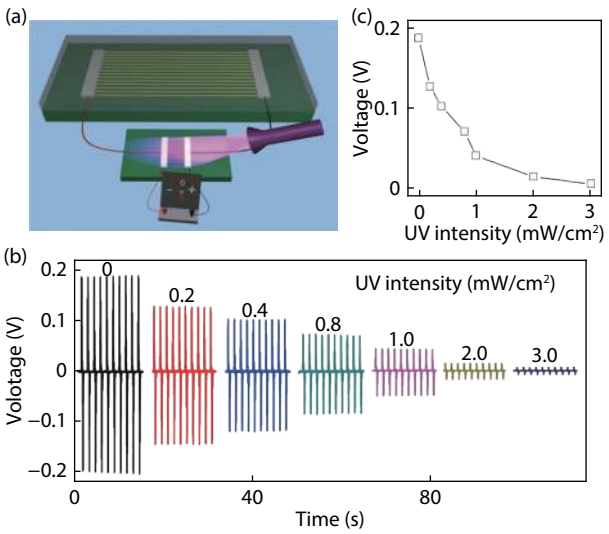

Fig. 13. (Color online) (a) The schematic of the FTNG integrated UV detector. (b) Photoresponse of the UV detector with different UV intensity. (c) Plot of UV detector voltage against the UV intensity. Reprinted from Ref. [127] with permission, Copyright 2012, American Chemical Society.

creating a p–n junction, creating a Schottky Junction by band alignment engineering[95, 99] or creating a semiconductor/graphene nanostructure[5]. Using the photovoltaic effect of these junctions, the energy can be harnessed upon the illumination of the light while detecting the photocurrent at the same time. One interesting report by Cao *et al.* using a polarization P(VDF-TrFE) layer to create a ferroelectric field one the perovskite NW and greatly enhanced the optoelectronic performance[112].

Power source integration is another way to produce self-powered photodetector. The power source can be micro/nanosolar cell, nanogenerator or other energy-storage devices (capacitor). Flexible transparent nanogenerator (FTNG) was integrated into a UV sensing unit as the power source[127]. The ZnO NWs UV sensors were powered by the FTNG and showed the typical response of a UV sensor with and without the illumination (Fig. 13(a)–13(c)). Shen's group, on the other hand, demonstrated integrating the supercapacitor and NW-based photodetector in the same system[128–130]. Those demonstrations is important for future development of highly-compacted flexible photodetection system.

One interesting report demonstrated the use of the wireless charging method to recharge the on-substrate capacitor. Yue *et al.* integrated a microsupercapacitor, a perovskite NW photodetector and a wireless charging coil on the same flexible substrate[131]. The report demonstrated a stable photocurrent detection after 7000 cycles as the photosensing unit is empowered by the constant charging by the microsupercapacitor which is constantly recharge by the wireless charging unit.

5. Conclusion and outlook

In this review, we have gone through the recent development of the NW-based flexible photodetector in terms of NW growth and assembly on flexible substrate, the development of individual materials group and the integration into a more complex system. Some material group shows substantial improvement in terms of NW growth, assembly and performance. Also, novel applications like image sensor and self-powered photodetector are demonstrated which are promising for the future use in different fields.

Despite all the positive research output, it is not hard to foresee that the development of the NW-based flexible photodetector still has a lot of room to grow. For example, some materials, like III–V NWs, are frequently grown under high-temperature process. A transfer step is necessary to applied on flexible substrate. However, the NWs alignment is usually not in perfect order and overlapped with each other. For some 1D nanostructure, like CNT and some metal oxide NW, the overlapped can be tolerated as they can form a NW network structure and still have good performance. But for some material systems, like III–V NWs, the bad alignment sometimes sabotages the performance because it complicates the charge transfer process. Especially when constraining the pixel size further toward smaller size, alignment fault will take a bigger role on the device performance. Therefore, better NW growth or NW array assembly technique is necessary to be developed.

Developing heterostructure is another point of emphasis that is having more and more attention in developing flexible photodetector. Combining NWs with other novel materials with excellent optoelectronic properties can enhance the device performance and the spectral absorption range. Non-1D nanostructure materials like C_{60}[51], graphene[75], semiconductor QDs[94], bulk perovskite film on fiber[99] and ferroelectric polymer[112] have been integrated as the heterostructure to enhance the device performance. Also, complicated structure like core-multishell NW structure has also been investigated and shows some promising result[25]. We expect more effort will be put to investigate the NW heterostructure like combining with other novel 2D nanostructure like 2D metal dichalcogenides (MoS_2, black phosphorus and etc.) or complicated NW structure like dot-in-wire and core-multishell NW for flexible photodetector integration. Also, more innovative process to combine these materials and/or smarter device structure design to maximize the performance of flexible electronics.

Large area fabrication is another challenging issue that is faced by flexible photodetector production. Despite of the development of the NW assembly techniques, most of them have either high production cost or high production time. The homogeneity of the transfer NW array is also hard to control in large area. Assembly techniques like inkjet printing and spray coating might be the solution of these issues but they are still facing the resolution problem that limits the pixel size of the image sensor and the ink of some materials is not yet developed. Directly growing the NWs on the flexible substrate is another potential solution but some flexible substrate like the polymer substrate simply cannot tolerate the high temperature NW growth process.

There are some issues that are commonly faced by flexible electronics that still needs better solution for real-life applications. For example, the mechanical durability demonstrated in most reports is up to hundreds of cycles and has certain degree of performance degradation. When considering the application of soft robotic that might have a higher bending frequency, the demonstrated performance might not match the need for these applications. Better packaging pro-

cess and device design is necessary. Other issues like the connection with the rigid data acquisition systems and long-term stability is still challenging[132]. Base on all the issues and challenges pointed out above, more efforts are needed for NW-based flexible photodetector forward to real-life integration.

Acknowledgments

We acknowledge the General Research Fund of the Research Grants Council of Hong Kong SAR, China (CityU 11211317), the National Natural Science Foundation of China (Grants 51672229), the Science Technology and Innovation Committee of Shenzhen Municipality (Grant JCYJ20170818095520778) and a grant from the Shenzhen Research Institute, City University of Hong Kong.

References

[1] Cheong P, Chang K F, Lai Y H, et al. A ZigBee-based wireless sensor network node for ultraviolet detection of flame. IEEE Trans Ind Electron, 2011, 58(11), 5271

[2] Yao S, Swetha P, Zhu Y. Nanomaterial-enabled wearable sensors for healthcare. Adv Healthc Mater, 2018, 7(1)

[3] Elgala H, Mesleh R, Haas H. Indoor optical wireless communication: Potential and state-of-the-art. IEEE Commun Mag, 2011, 49(9), 56

[4] Zhang M, Yeow J T W. Flexible polymer-carbon nanotube composite with high-response stability for wearable thermal imaging. ACS Appl Mater Interfaces, 2018, 10(31), 26604

[5] Peng L, Hu L, Fang X. Energy harvesting for nanostructured self-powered photodetectors. Adv Funct Mater, 2014, 24(18), 2591

[6] Xie C, Mak C, Tao X, et al. Photodetectors based on two-dimensional layered materials beyond graphene. Adv Funct Mater, 2017, 27(19), 1603886

[7] Buscema M, Island J O, Groenendijk D J, et al. Photocurrent generation with two-dimensional van der Waals semiconductors. Chem Soc Rev, 2015, 44(11), 3691

[8] Sun Z, Chang H. Graphene and graphene-like two-dimensional materials in photodetection: Mechanisms and methodology. ACS Nano, 2014, 8(5), 4133

[9] Dejarld M, Shin J C, Chern W, et al. Formation of high aspect ratio GaAs nanostructures with metal-assisted chemical etching. Nano Lett, 2011, 11, 5259

[10] Mohseni P K, Kim S H, Zhao X, et al. GaAs pillar array-based light emitting diodes fabricated by metal-assisted chemical etching. J Appl Phys, 2013, 114, 64909

[11] Lu W, Lieber C M. Semiconductor nanowires. J Phys D, 2006, 39, R387

[12] Yan R, Gargas D, Yang P. Nanowire photonics. Nat Photonics, 2009, 3, 569

[13] Dick K A, Deppert K, Martensson T, et al. Failure of the vapor-liquid-solid mechanism in Au-assisted MOVPE growth of InAs nanowires. Nano Lett, 2005, 5, 761

[14] Persson A, Larsson M, Stenstrom S, et al. Solid-phase diffusion mechanism for GaAs nanowire growth. Nat Mater, 2004, 3, 677

[15] Morales A M, Lieber C M. A laser ablation method for the synthesis of crystalline semiconductor nanowires. Science, 1998, 279, 208

[16] Colombo C, Spirkoska D, Frimmer M, et al. Ga-assisted catalyst-free growth mechanism of GaAs nanowires by molecular beam epitaxy. Phys Rev B, 2008, 77, 155326

[17] Han N, Wang F, Hui A T, et al. Facile synthesis and growth mechanism of Ni-catalyzed GaAs nanowires on non-crystalline substrates. Nanotechnology, 2011, 22, 285607

[18] Hui A T, Wang F, Han N, et al. High-performance indium phosphide nanowires synthesized on amorphous substrates: from formation mechanism to optical and electrical transport measurements. J Mater Chem, 2012, 22, 10704

[19] Yang Z X, Wang F, Han N, et al. Crystalline GaSb nanowires synthesized on amorphous substrates: From the formation mechanism to p-channel transistor applications. ACS Appl Mater Interfaces, 2013, 5, 10946

[20] Zhou Q, Park J G, Nie R, et al. Nanochannel-assisted perovskite nanowires: from growth mechanisms to photodetector applications. ACS Nano, 2018, 12, 8406

[21] Zhu H, Fu Y, Meng F, et al. Lead halide perovskite nanowire lasers with low lasing thresholds and high quality factors. Nat Mater, 2015, 14, 636

[22] Gholipour B, Adamo G, Cortecchia D, et al. Organometallic perovskite metasurfaces. Adv Mater, 2017, 29, 1604268

[23] Maceiczyk R M, Dumbgen K, Lignos I, et al. Microfluidic reactors provide preparative and mechanistic insights into the synthesis of formamidinium lead halide perovskite nanocrystals. Chem Mater, 2017, 29, 8433

[24] Lignos I, Maceiczyk R M, Demello A J. Microfluidic technology: uncovering the mechanisms of nanocrystal nucleation and growth. Acc Chem Res, 2017, 50, 1248

[25] Zhang H, Dai X, Guan N, et al. Flexible photodiodes based on nitride core/shell p–n junction nanowires. ACS Appl Mater Interfaces, 2016, 8, 26198

[26] Takahashi T, Takei K, Adabi E, et al. Parallel array InAs nanowire transistors for mechanically bendable, ultrahigh frequency electronics. ACS Nano, 2010, 4, 5855

[27] Fan Z, Ho J C, Takahashi T, et al. Toward the development of printable nanowire electronics and sensors. Adv Mater, 2009, 21, 3730

[28] Fan Z, Ho J C, Jacobson Z A, et al. Wafer-scale assembly of highly ordered semiconductor nanowire arrays by contact printing. Nano Lett, 2008, 8, 20

[29] Hou J J, Han N, Wang F, et al. Synthesis and characterizations of ternary InGaAs nanowires by a two-step growth method for high-performance electronic devices. ACS Nano, 2012, 6, 3624

[30] Li D, Lan C, Manikandan A, et al. Ultra-fast photodetectors based on high-mobility indium gallium antimonide nanowires. Nat Commun, 2019, 10, 1664

[31] Assad O, Leshansky A, Wang B, et al. Spray-coating route for highly aligned and large-scale arrays of nanowires. ACS Nano, 2012, 6, 4702

[32] Lee J, Shin D, Park J. Fabrication of silver nanowire-based stretchable electrodes using spray coating. Thin Solid Films, 2016, 608, 34

[33] Binda M, Natali D, Iacchetti A, et al. Integration of an organic photodetector onto a plastic optical fiber by means of spray coating technique. Adv Mater, 2013, 25(31), 4335

[34] Park S, Kim S J, Nam J H, et al. Significant enhancement of infrared photodetector sensitivity using a semiconducting single-walled carbon nanotube/C_{60} phototransistor. Adv Mater, 2015, 27, 759

[35] Konstantatos G, Clifford J, Levina L, et al. Sensitive solution-processed visible-wavelength photodetectors. Nat Photonics, 2007, 1(9), 531

[36] Konstantatos G, Howard I, Fischer A, et al. Ultrasensitive solution-cast quantum dot photodetectors. Nature, 2006, 442(7099), 180

[37] Mueller T, Xia F, Avouris P. Graphene photodetectors for high-speed optical communications. Nat Photonics, 2010, 4(5), 297

[38] Xia F, Mueller T, Lin Y M, et al. Ultrafast graphene photodetector. Nat Nanotechnol, 2009, 4, 839

[39] Liu Y, Wang F, Wang X, et al. Planar carbon nanotube–graphene hybrid films for high-performance broadband photodetectors. Nat Commun, 2015, 6, 8589

[40] Xie J, Liu W, Macewan M R, et al. Neurite outgrowth on electrospun nanofibers with uniaxial alignment: the effects of fiber density, surface coating, and supporting substrate. ACS Nano, 2014, 8, 1878
[41] Hu X, Zhang X, Liang L, et al. High-performance flexible broadband photodetector based on organolead halide perovskite. Adv Funct Mater, 2014, 24(46), 7373
[42] Wu H, Sun Y, Lin D, et al. GaN Nanofibers based on electrospinning: facile synthesis, controlled assembly, precise doping, and application as high performance UV photodetector. Adv Mater, 2009, 21, 227
[43] Zheng Z, Gan L, Zhai T. Electrospun nanowire arrays for electronics and optoelectronics. Sci Chin Mater, 2016, 59, 200
[44] Liu X, Gu L, Zhang Q, et al. All-printable band-edge modulated ZnO nanowire photodetectors with ultra-high detectivity. Nat Commun, 2014, 5, 4007
[45] Li D, Wang Y, Xia Y. Electrospinning nanofibers as uniaxially aligned arrays and layer-by-layer stacked films. Adv Mater, 2004, 16, 361
[46] Dai X, Messanvi A, Zhang H, et al. Flexible light-emitting diodes based on vertical nitride nanowires. Nano Lett, 2015, 15, 6958
[47] Richter M, Heumüller T, Matt G J, et al. Carbon photodetectors: the versatility of carbon allotropes. Adv Energy Mater, 2017, 7(10)
[48] Barkelid M, Zwiller V. Photocurrent generation in semiconducting and metallic carbon nanotubes. Nat Photonics, 2014, 8(1), 47
[49] Siitonen A J, Tsyboulski D A, Bachilo S M, et al. Dependence of exciton mobility on structure in single-walled carbon nanotubes. J Phys Chem Lett, 2010, 1(14), 2189
[50] Chen K, Gao W, Emaminejad S, et al. Printed carbon nanotube electronics and sensor systems. Adv Mater, 2016, 28(22), 4397
[51] Zhang S, Cai L, Wang T, et al. Fully printed flexible carbon nanotube photodetectors. Appl Phys Lett, 2017, 110(12)
[52] Rogalski A, Chrzanowski K. Infrared devices and techniques. Metrol Meas Syst, 2014, 21(4), 565
[53] Liu Y, Wei N, Zeng Q, et al. Room temperature broadband infrared carbon nanotube photodetector with high detectivity and stability. Adv Opt Mater, 2016, 4(2), 238
[54] Huang Z, Gao M, Yan Z, et al. Flexible infrared detectors based on p–n junctions of multi-walled carbon nanotubes. Nanoscale, 2016, 8(18), 9592
[55] Takahashi T, Yu Z, Chen K, et al. Carbon nanotube active-matrix backplanes for mechanically flexible visible light and X-ray imagers. Nano Lett, 2013, 13(11), 5425
[56] Suzuki D, Oda S, Kawano Y. A flexible and wearable terahertz scanner. Nat Photonics, 2016, 10(12), 809
[57] Liu Y, Liu Y, Qin S, et al. Graphene-carbon nanotube hybrid films for high-performance flexible photodetectors. Nano Res, 2017, 10(6), 1880
[58] Pradhan B, Setyowati K, Liu H, et al. Carbon nanotube-polymer nanocomposite infrared sensor. Nano Lett, 2008, 8(4), 1142
[59] Hou W, Zhao N J, Meng D, et al. Controlled growth of well-defined conjugated polymers from the surfaces of multiwalled carbon nanotubes: photoresponse enhancement via charge separation. ACS Nano, 2016, 10(5), 5189
[60] Sarker B K, Arif M, Khondaker S I. Near-infrared photoresponse in single-walled carbon nanotube/polymer composite films. Carbon, 2010, 48(5), 1539
[61] Pyo S, Kim W, Jung H Il, et al. Heterogeneous integration of carbon-nanotube–graphene for high-performance, flexible, and transparent photodetectors. Small, 2017, 13(27), 1700918
[62] Du J, Pei S, Ma L, et al. Carbon nanotube- and graphene-based transparent conductive films for optoelectronic devices. Adv Mater, 2014, 26(13), 1958
[63] Kim D H, Ahn J H, Won M C, et al. Stretchable and foldable silicon integrated circuits. Science, 2008, 320(5875), 507
[64] Huang Z, Geyer N, Werner P, et al. Metal-assisted chemical etching of silicon: A review. Adv Mater, 2011, 23(2), 285
[65] Mulazimoglu E, Coskun S, Gunoven M, et al. Silicon nanowire network metal–semiconductor–metal photodetectors. Appl Phys Lett, 2013, 103(8), 083114
[66] Kim D H, Lee W, Myoung J M. Flexible multi-wavelength photodetector based on porous silicon nanowires. Nanoscale, 2018, 10(37), 17705
[67] Hossain M, Kumar G S, Barimar Prabhava S N, et al. Transparent, flexible silicon nanostructured wire networks with seamless junctions for high-performance photodetector applications. ACS Nano, 2018, 12(5), 4727
[68] Shen L, Pun E Y B, Ho J C. Recent developments in III–V semiconducting nanowires for high-performance photodetectors. Mater Chem Front, 2017, 1, 630
[69] Miao J, Hu W, Guo N, et al. Single InAs nanowire room-temperature near-infrared photodetectors. ACS Nano, 2014, 8, 3628
[70] Han N, Yang Z X, Wang F, et al. High-performance GaAs nanowire solar cells for flexible and transparent photovoltaics. ACS Appl Mater Interfaces, 2015, 7(36), 20454
[71] Yang Z, Han N, Fang M, et al. Surfactant-assisted chemical vapour deposition of high-performance small-diameter GaSb nanowires. Nat Commun, 2014, 5, 5249
[72] Duan T, Liao C, Chen T, et al. Single crystalline nitrogen-doped InP nanowires for low-voltage field-effect transistors and photodetectors on rigid silicon and flexible mica substrates. Nano Energy, 2015, 15, 293
[73] Luo T, Liang B, Liu Z, et al. Single-GaSb-nanowire-based room temperature photodetectors with broad spectral response. Sci Bull, 2015, 60, 101
[74] Royo M, De Luca M, Rurali R, et al. A review on III–V core–multishell nanowires: growth, properties, and applications. J Phys D, 2017, 50, 143001
[75] Han S, Lee S K, Choi I, et al. Highly efficient and flexible photosensors with GaN nanowires horizontally embedded in a graphene sandwich channel. ACS Appl Mater Interfaces, 2018, 10(44), 38173
[76] Lapierre R R, Robson M, Azizur-Rahman K M, et al. A review of III-V nanowire infrared photodetectors and sensors. J Phys D, 2017, 50(12), 123001
[77] Hua M, Zhang S, Pan B, et al. Heavy metal removal from water/wastewater by nanosized metal oxides: a review. J Hazard Mater, 2012, 211, 317
[78] Zou Y, Zhang Y, Hu Y, et al. Ultraviolet detectors based on wide bandgap semiconductor nanowire: A review. Sensors, 2018, 18(7), 2072
[79] Sun Y F, Liu S B, Meng F L, et al. Metal oxide nanostructures and their gas sensing properties: A review. Sensors, 2012, 12(3), 2610
[80] Wong H S P, Lee H Y, Yu S, et al. Metal-oxide RRAM. Proc IEEE, 2012, 100(6), 1951
[81] Zheng Z, Gan L, Zhang J B, et al. An enhanced UV-Vis-NIR an d flexible photodetector based on electrospun Zno nanowire array/PbS quantum dots film heterostructure. Adv Sci, 2017, 4(3), 1600316
[82] Wang S, Sun H, Wang Z, et al. In situ synthesis of monoclinic β-Ga_2O_3 nanowires on flexible substrate and solar-blind photodetector. J Alloys Compd, 2019, 787(30), 133
[83] Liu Z, Huang H, Liang B, et al. Zn_2GeO_4 and $In_2Ge_2O_7$ nanowire mats based ultraviolet photodetectors on rigid and flexible substrates. Opt Express, 2012, 20, 2982
[84] Mallampati B, Nair S V, Ruda H E, et al. Role of surface in high photoconductive gain measured in ZnO nanowire-based photodetector. J Nanoparticle Res, 2015, 17(4), 176
[85] Alsultany F H, Hassan Z, Ahmed N M. A high-sensitivity, fast-re-

sponse, rapid-recovery UV photodetector fabricated based on catalyst-free growth of ZnO nanowire networks on glass substrate. Opt Mater, 2016, 60, 30

[86] Zhao X, Wang F, Shi L, et al. Performance enhancement in ZnO nanowire based double Schottky-barrier photodetector by applying optimized Ag nanoparticles. RSC Adv, 2016, 6(6), 4634

[87] Liu J, Lu R, Xu G, et al. Development of a seedless floating growth process in solution for synthesis of crystalline ZnO micro/nanowire arrays on graphene: Towards high-performance nanohybrid ultraviolet photodetectors. Adv Funct Mater, 2013, 23(39), 4941

[88] Wu J M, Chen Y R, Lin Y H. Rapidly synthesized ZnO nanowires by ultraviolet decomposition process in ambient air for flexible photodetector. Nanoscale, 2011, 3(3), 1053

[89] Liu J, Wu W, Bai S, et al. Synthesis of high crystallinity ZnO nanowire array on polymer substrate and flexible fiber-based sensor. ACS Appl Mater Interfaces, 2011, 3(11), 4197

[90] Zheng Z, Gan L, Li H, et al. A fully transparent and flexible ultraviolet-visible photodetector based on controlled electrospun ZnO–CdO heterojunction nanofiber arrays. Adv Funct Mater, 2015, 25(37), 5885

[91] Manekkathodi A, Lu M Y, Wang C W, et al. Direct growth of aligned zinc oxide nanorods on paper substrates for low-cost flexible electronics. Adv Mater, 2010, 22(36), 4059

[92] Li L, Gu L, Lou Z, et al. ZnO Quantum dot decorated Zn_2SnO_4 nanowire heterojunction photodetectors with drastic performance enhancement and flexible ultraviolet image sensors. ACS Nano, 2017, 11(4), 4067

[93] Shen X, Duan L, Li J, et al. Enhanced performance of flexible ultraviolet photodetectors based on carbon nitride quantum dot/ZnO nanowire nanocomposites. Mater Res Express, 2019, 6(4), 045002

[94] Li L, Lou Z, Shen G. Flexible broadband image sensors with SnS quantum dots/Zn_2SnO_4 nanowires hybrid nanostructures. Adv Funct Mater, 2018, 28(6), 1705389

[95] Dong Y, Zou Y, Song J, et al. Self-powered fiber-shaped wearable omnidirectional photodetectors. Nano Energy, 2016, 30, 173

[96] Wang X, Liu B, Liu R, et al. Fiber-based flexible all-solid-state asymmetric supercapacitors for integrated photodetecting system. Angew Chemie, 2014, 53(7), 1849

[97] Zhang F, Niu S, Guo W, et al. Piezo-phototronic effect enhanced visible/UV photodetector of a carbon-fiber/ZnO-CdS double-shell microwire. ACS Nano, 2013, 7(5), 4537

[98] Wang S, Zou Y, Shan Q, et al. Nanowire network-based photodetectors with imaging performance for omnidirectional photodetecting through a wire-shaped structure. RSC Adv, 2018, 8(59), 3666

[99] Sun H, Tian W, Cao F, et al. Ultrahigh-performance self-powered flexible double-twisted fibrous broadband perovskite photodetector. Adv Mater, 2018, 30(21), 1706986

[100] Xie X, Shen G. Single-crystalline In_2S_3 nanowire-based flexible visible-light photodetectors with an ultra-high photoresponse. Nanoscale, 2015, 7, 5046

[101] Graham R, Miller C, Oh E, et al. Electric field dependent photocurrent decay length in single lead sulfide nanowire field effect transistors. Nano Lett, 2011, 11(2), 717

[102] Li L, Lou Z, Shen G. Hierarchical CdS nanowires based rigid and flexible photodetectors with ultrahigh sensitivity. ACS Appl Mater Interfaces, 2015, 7, 23507

[103] Chen G, Wang W, Wang C, et al. Controlled synthesis of ultrathin Sb_2Se_3 nanowires and application for flexible photodetectors. Adv Sci, 2015, 2(10), 1500109

[104] Liang Y, Wang Y, Wang J, et al. High-performance flexible photodetectors based on single-crystalline Sb_2Se_3 nanowires. RSC Adv, 2016, 6(14), 11501

[105] Hu W, Huang W, Yang S, et al. High-performance flexible photodetectors based on high-quality perovskite thin films by a vapor–solution method. Adv Mater, 2017, 29(43), 1703256

[106] Bao C, Zhu W, Yang J, et al. Highly flexible self-powered organolead trihalide perovskite photodetectors with gold nanowire networks as transparent electrodes. ACS Appl Mater Interfaces, 2016, 8(36), 23868

[107] Yang W S, Park B W, Jung E H, et al. Iodide management in formamidinium-lead-halide-based perovskite layers for efficient solar cells. Science, 2017, 356(6345), 1376

[108] Chen Q, De Marco N, Yang Y, et al. Under the spotlight: The organic-inorganic hybrid halide perovskite for optoelectronic applications. Nano Today, 2015, 10(3), 355

[109] Xu X, Zhang X X, Deng W, et al. Saturated vapor-assisted growth of single-crystalline organic-inorganic hybrid perovskite nanowires for high-performance photodetectors with robust stability. ACS Appl Mater Interfaces, 2018, 10(12), 10287

[110] Asuo I M, Fourmont P, Ka I, et al. Highly efficient and ultrasensitive large-area flexible photodetector based on perovskite nanowires. Small, 2019, 15(1), 1804150

[111] Zhu B S, He Z, Yao J S, et al. Potassium ion assisted synthesis of organic–inorganic hybrid perovskite nanobelts for stable and flexible photodetectors. Adv Opt Mater, 2018, 6(3), 1701029

[112] Cao F, Tian W, Wang M, et al. Semitransparent, flexible, and self-powered photodetectors based on ferroelectricity-assisted perovskite nanowire arrays. Adv Funct Mater, 2019, 1901280

[113] Meng Y, Lan C, Li F, et al. Direct vapor–liquid–solid synthesis of all-inorganic perovskite nanowires for high-performance electronics and optoelectronics. ACS Nano, 2019, 13(5), 6060

[114] Zhou Y, Luo J, Zhao Y, et al. Flexible linearly polarized photodetectors based on all-inorganic perovskite $CsPbI_3$ nanowires. Adv Opt Mater, 2018, 6(22), 1800679

[115] Kaplan H. Practical applications of infrared thermal sensing and imaging equipment. 3rd ed. SPIE Press, 2007

[116] Song Y M, Xie Y, Malyarchuk V, et al. Digital cameras with designs inspired by the arthropod eye. Nature, 2013, 497(7447), 95

[117] Krauss T C, Warlen S C. The forensic science use of reflective ultraviolet photography. J Forensic Sci, 1985, 30(1), 262

[118] Fulton J E. Utilizing the ultraviolet (UV detect) camera to enhance the appearance of photodamage and other skin conditions. Dermatologic Surg, 1997, 23(3), 163

[119] Wilkes T C, McGonigle A J S, Pering T D, et al. Ultraviolet imaging with low cost smartphone sensors: Development and application of a raspberry pi-based UV camera. Sensors, 2016, 16(10), 1649

[120] Fingas M, Brown C. Review of oil spill remote sensing. Mar Pollut Bull, 2014, 83(1), 9

[121] Zhou W, Li H, Yi X, et al. A criterion for UV detection of AC corona inception in a rod-plane air gap. IEEE Trans Dielectr Electr Insul, 2011, 18(1), 232

[122] Gade R, Moeslund T B. Thermal cameras and applications: A survey. Mach Vis Appl, 2014, 25(1), 245

[123] Zhang Q, Lin Y, Tsui K H, et al. 3D arrays of 1024-pixel image sensors based on lead halide perovskite nanowires. Adv Mater, 2016, 28(44), 9713

[124] Fan Z, Kapadia R, Leu P W, et al. Ordered arrays of dual-diameter nanopillars for maximized optical absorption. Nano Lett, 2010, 10(10), 3823

[125] Deng W, Zhang X, Huang L, et al. Aligned single-crystalline perovskite microwire arrays for high-performance flexible image sensors with long-term stability. Adv Mater, 2016, 28, 2201

[126] Xu S, Qin Y, Xu C, et al. Self-powered nanowire devices. Nat Nanotechnol, 2010, 5(5), 366

[127] Wu W, Bai S, Yuan M, et al. Lead zirconate titanate nanowire textile nanogenerator for wearable energy-harvesting and self-

powered devices. ACS Nano, 2012, 6(7), 6231

[128] Gu S, Lou Z, Li L, et al. Fabrication of flexible reduced graphene oxide/Fe_2O_3 hollow nanospheres based on-chip micro-supercapacitors for integrated photodetecting applications. Nano Res, 2016, 9(2), 424

[129] Wang X, Liu B, Wang Q, et al. Three-dimensional hierarchical $GeSe_2$ nanostructures for high performance flexible all-solid-state supercapacitors. Adv Mater, 2013, 25(10), 1479

[130] Xu J, Shen G. A flexible integrated photodetector system driven by on-chip microsupercapacitors. Nano Energy, 2015, 13, 131

[131] Yue Y, Yang Z, Liu N, et al. A flexible integrated system containing a microsupercapacitor, a photodetector, and a wireless charging coil. ACS Nano, 2016, 10, 11249

[132] Costa J C, Spina F, Lugoda P, et al. Flexible sensors—from materials to applications. Technologies, 2019, 7, 35